Journal of Energy Storage 73 (2023) 108909

Contents lists available at ScienceDirect

Journal of Energy Storage

journal homepage: www.elsevier.com/locate/est

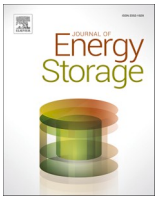

Research papers

Resilience of hydrogen fuel station-integrated power systems with high penetration of photovoltaics

Wenqing Cai [a], Seyed Amir Mansouri [b], Ahmad Rezaee Jordehi [c,*], Marcos Tostado-Véliz [d], Amir Ahmarinejad [e], Francisco Jurado [d]

[a] School of Science, Anhui Agricultural University, Hefei 230036, China
[b] Institute for research in technology (IIT), Comillas Pontifical University, 28015 Madrid, Spain
[c] Department of Electrical Engineering, Rasht Branch, Islamic Azad University, Rasht, Iran
[d] Department of Electrical Engineering, University of Jaén, 23700 Linares, Spain
[e] Department of Electrical Engineering, Central Tehran Branch, Islamic Azad University, Tehran, Iran

ARTICLE INFO

Keywords:
Electrolyzer
Green hydrogen
Hydrogen fuel station
Hydrogen storage
Mobile battery
Power system resilience

ABSTRACT

Hydrogen fuel stations (HFSs) may be connected to power systems; to absorb electricity, produce hydrogen and supply hydrogen demands. To the best of the authors' knowledge, the resilience of HFS-integrated power systems has not been addressed in the literature. In this research, a novel strategy is proposed for resilience enhancement of PV-rich HFS-integrated power systems, considering the uncertainties. In the proposed strategy, fuel cells (FCs) and hydrogen tanks are added to HFSs and mobile batteries are added to the power system. A two-stage stochastic model is developed in which the location of mobile batteries are the first-stage here-and-now decision variables and other variables are second-stage wait-and-see decision variables. The model is formulated as a multi-objective problem as the ability of the system to supply both electricity and hydrogen demands are considered. Expected load not served (ELNS) is used as resilience metric. Case study is a modified IEEE 24-bus power system with 5 HFSs. The results confirm that with the proposed resilience enhancement strategy, hurricane does not result in any shed for hydrogen demands. As per results, mobile batteries are the most efficient tools in resilience enhancement of the studied system; they cause 84 % improvement in ELNS of electricity and 43 % improvement in ELNS of hydrogen. The results also show that besides mobile batteries, hydrogen storage tanks and FCs are the most efficient components in resilience enhancement of the system. Hydrogen tanks improve ELNS of electricity by 1.8 % and remove the need of system operator to shed hydrogen demands. A sensitivity analysis is done to see how the results of the developed model are sensitive to its parameters.

1. Introduction

The consumption of hydrogen in different sectors is increasing [1–3]. The largest share of hydrogen demand is from chemical sectors for ammonia production and in refining industries for desulphurization of fuels [4]; it may be used in transportation sector for charging fuel cell electric vehicles and may also be used for residential heating and production of steel, iron and glass [4–6]. The electricity fed into electrolyzers may be produced by fossil fuel-based generators or renewable energy resources. The hydrogen produced through renewable energy resources is referred to as green hydrogen. Green hydrogen offers a couple of benefits [4,7–10]; it decreases emissions and is a big step towards decarbonization; decreases renewable energy curtailment and enables the linkage to other energy sectors.

With proliferation of hydrogen production units and hydrogen demands, they are commonly integrated into power systems. Hydrogen fuel stations (HFSs) which typically include electrolyzers and hydrogen tanks are connected to buses of power systems; they absorb electricity from local bus and supply hydrogen demands in the neighborhood. The integration of HFSs/electrolyzers adds to the flexibility of power systems, however they may cause new challenges for power system operators and pose new research questions.

In literature, the impact of HFSs and electrolyzers on power systems has been investigated in some researches.

In [11], a stochastic mixed-integer linear programming (MILP) model is developed for the optimal placement HFSs in power systems with high penetration of renewable energy resources, while power

* Corresponding author.
E-mail address: ahmadrezaeejordehi@gmail.com (A. Rezaee Jordehi).

https://doi.org/10.1016/j.est.2023.108909
Received 16 January 2023; Received in revised form 15 August 2023; Accepted 2 September 2023

Nomenclature

Acronyms

FC	Fuel cell
HFS	Hydrogen fuel station
MILP	Mixed-integer linear programming
PV	Photovoltaic

Sets

$\Omega_i^{connectbus}$	Set of buses connected to bus i
ref	Reference bus
Ω_i^{g}	Set of generators at bus i
Ω_i^{PV}	Set of PVs at bus i
$fail$	Set of failed lines
$nofail$	Set of non-failed lines

Bars

$\underline{*}$	Lower bound
$\overline{*}$	Upper bound

Indices

bat	Fixed battery
ch/dch	Charging/discharging status of storage systems
EL	Electrolyzer
e	Electric
FC	FC
g	Generator
h	Hydrogen
i,j	Bus
in	Initial value
hfs	HFS
MB	Mobile battery
PV	PV
s	Scenario
$shed$	Shed
t	Time
$tank$	Hydrogen tank

Parameters and variables

η	Battery efficiency
CR	Conversion ratio (for electrolyzers and FCs)
$conex$	Connection status of buses (1 for connected ones)
D	Demand
$ELNS$	Expected load not supplied
E	State of charge of storage system
H	Hydrogen (kg)
u	ON/OFF status
J	Objective (weighted sum of ELNS of electricity and hydrogen)
P	Power
Fl	Power flow
α	Probability (of reduced scenarios)
β	Phase angle of bus voltage
RU	Ramp-up limit
RD	Ramp-down limit
X	Reactance of transmission line
Δt	Time resolution
μ	The existence status of mobile battery at a bus
$Tshed$	Total demand shed
W	Weight in multi-objective optimisation

system operator sells its extra hydrogen in a day-ahead local hydrogen market. In the developed model, a linearisation strategy is used to transform the nonlinear binary terms into linear terms and the uncertainties of electricity and hydrogen demands, PV generation and hydrogen market prices are considered.

In [12], a stochastic MILP model has been proposed for optimal participation of HFSs in electricity markets with uncertain electricity prices, while HFS operator may choose among different types of contracts and markets. In [13], HFSs have been integrated into power systems and a new structure has been proposed for hydrogen exchange through transportation system. The results show that the proposed structure is compatible with multi-energy carrier markets. In [14], optimal design of HFSs has been done within renewable-rich power systems.

In [15], the impact of electrolyzers and hydrogen demands on available transmission capacity has been evaluated in power systems with electricity and hydrogen demands and high level of wind penetration. A nonlinear AC load flow model has been used. The results show significant impact of size and location of electrolyzers as well as wind penetration level on harvestable hydrogen. As per the achieved results, for a certain electrolyzer size, the harvestable hydrogen decreases in higher loading margins.

In [16], a security-constrained optimal power flow has been done for power systems with electricity and hydrogen demands. Electrolyzers and hydrogen storage tanks have been used to produce hydrogen and deliver it to hydrogen demands. The results show that the integration of hydrogen demands and electrolyzers increase the profit of power system operator as they decrease the curtailment cost of renewables. In [17], hydrogen demands and electrolyzers have been integrated into a power system to decrease the renewable energy curtailment induced by retirement of 16 GW conventional fossil-fueled power plants and addition of 65 GW renewable power generation in Spain. In [18], the Europe's potential to supply hydrogen demand by renewable energy has been assessed and concluded that the whole hydrogen demand of the Europe may be supplied by renewable generators.

In [19], a bi-level model has been proposed for operational equilibrium of power, transportation and hydrogen systems. In the proposed bi-level model, the upper-level problem minimises the cost of hydrogen fuel stations and decides the electrolyzer load and hydrogen prices; on the other hand, power system and transportation system are at the lower level in which electricity demands and hydrogen prices are determined. For traffic system, a traffic assignment problem is solved to determine hydrogen demand.

In [20], operational planning has been done for HFSs including Alkaline electrolyzer, low-pressure storage and compressor, connected to both electricity markets and wind power plants. The objective is to minimise HFS planning cost and maximise the utilisation of wind electricity. The results show that the reduction of taxes and surcharges considerably changes the planning outcomes. In [21], optimal investment has been done for electrolyzers and hydrogen storage systems connected to a power system. The electrolyzer and storage system aim to supply industrial hydrogen demands in Sichuan Province, China. The results confirm that if the electrolyzers are installed close to hydrogen demands, their utilisation factor may be increased by 10 %.

In [22], a MILP model has been developed for operational planning of proton-exchange membrane (PEM) electrolyzers. The model determines the electricity purchased from power system or photovoltaic (PV) units as well as the purchased reformed hydrogen. The developed model minimises operation cost and emissions, while maximises the share of green hydrogen. In [23], operational planning has been done for a hybrid electricity-hydrogen system including battery, wind turbines, PV, electrolyzer, ammonia plant, methanol plant and biogas plant.

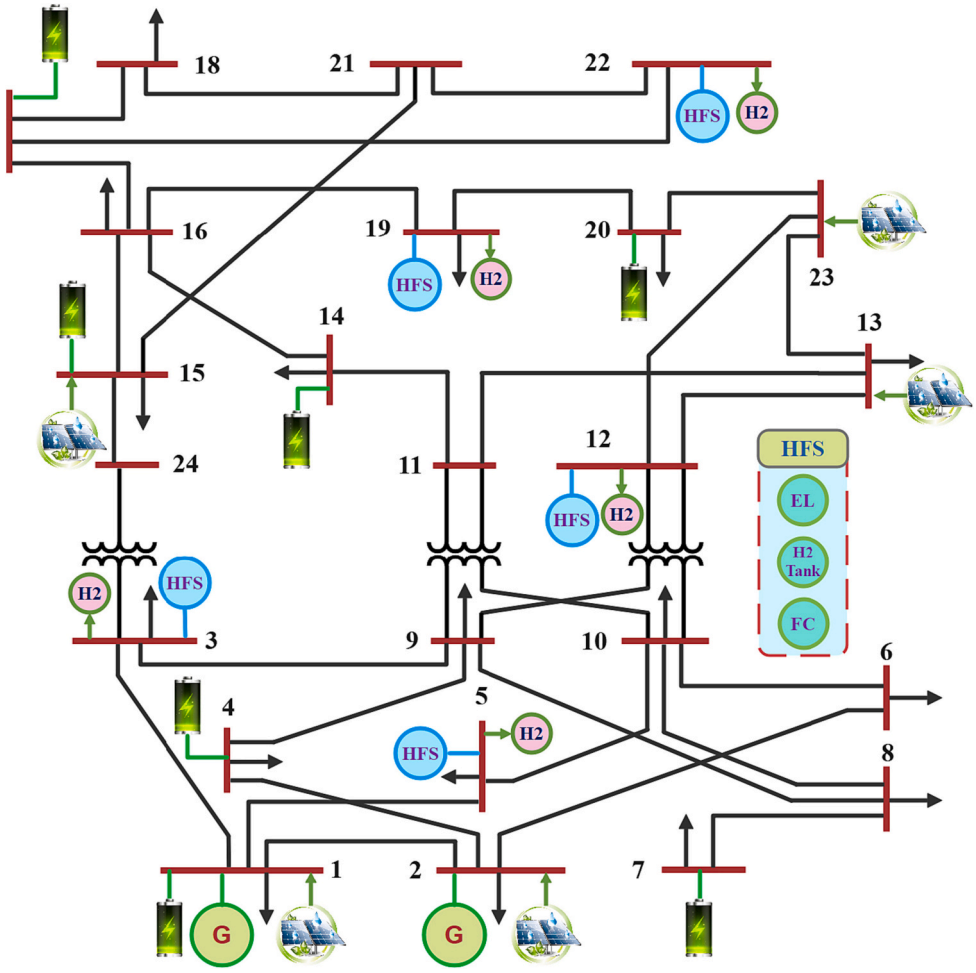

Fig. 1. Case study.

Despite the above-mentioned researches on power systems with hydrogen production units and hydrogen demands, to the best of the authors' knowledge, the resilience enhancement of those systems have not been addressed. The resilience of a power system is defined as its ability to withstand extreme events and maintain continuous supply of demands [24]. Extreme events such as hurricane and flood are low-probable, high impact events which may lead to the simultaneous outage of multiple power system components and result in the interruption of supply for lots of consumers [24]. Enhancement of the resilience in power and energy systems results in significant saving through expenditure recovery and risk reduction [24,25]. Resilience enhancement measures may be subdivided into two categories; power system hardening and operational measures [24,26].

In this research, a novel strategy has been proposed for resilience enhancement of HFS-integrated power systems with high PV penetration and high storage capacity, considering the uncertainties in the failed lines, failure times and repair times. In the proposed strategy, fuel cells (FCs) are added to HFSs and mobile batteries are added to the power system. A two-stage stochastic model has been developed in which the location of mobile batteries are first-stage here-and-now decision variables and other variables are second-stage wait-and-see decision variables. The model has been formulated as a multi-objective problem as the ability of the system to supply both electricity and hydrogen demands are considered. Expected load not served (ELNS) has been used as resilience metric. The contributions of this research are listed as below.

- ✓ A two-stage stochastic model has been developed with both here-and-now and wait-and-see decision variables considering the uncertainties of failed transmission lines, their failure and repair times.
- ✓ FCs have been added to HFSs to enhance the resilience of the system.
- ✓ Mobile batteries have been incorporated into power system to enhance its resilience.
- ✓ The effect of the size and number of mobile batteries on system resilience has been assessed.
- ✓ The effect of weights in the developed bi-objective model on resilience metrics has been assessed.

2. The proposed model

As Fig. 1 shows, the case study is a modified IEEE 24-bus power system in which 5 HFSs are installed in buses 3, 5, 12, 19 and 22; 7 fixed batteries are installed in buses 1, 4, 7, 14, 15, 17 and 20; 5 PV power plants are installed at buses 1, 2, 13, 15 and 23. The system includes only 2 dispatchable generators and the penetration of PV is high. Each HFS includes an electrolyzer, a hydrogen storage tank and a fuel cell. The data of IEEE 24-bus power system has been taken from [27]. The proposed two-stage stochastic model for resilience enhancement of the HFS-integrated power system is characterised by Eqs. (1)–(43).

As system includes both electricity and hydrogen demands, the objective of the model is defined as a linear weighted sum of ELNS of electricity and hydrogen, represented by Eq. (1). ELNS of electricity is defined by Eqs. (2)–(3) [24]; in a similar way, ELNS for hydrogen demands is defined by Eqs. (4)–(5). Deciding on the values of weight factors W_e and W_h is the sole responsibility of the system operator.

$$J = W_e ELNS_e + W_h ELNS_h \tag{1}$$

$$Tshed_{e,s} = \sum_i \sum_t P_{shed,i,t,s} \Delta t \forall s \tag{2}$$

$$ELNS_e = \sum_S \alpha_s Tshed_{e,s} \tag{3}$$

$$Tshed_{h,s} = \sum_i \sum_t H_{shed,i,t,s} \forall s \tag{4}$$

$$ELNS_h = \sum_S \alpha_s Tshed_{h,s} \tag{5}$$

The flow of power in the system is constrained by Eqs. (6)–(10) which includes DC load flow equations [24]. According to Eq. (6), the flow of each line is proportional to the difference between phase angles of the connected buses and inversely proportional to its reactance. As per Eq. (7), the flow of each failed line is equal to zero and Eq. (8) imposes upper and lower bounds on the flow of lines. Constraints (9) set the phase angle of the reference bus as zero.

$$Fl_{i,j,t,s} = \frac{(\beta_{i,t,s} - \beta_{j,t,s})}{X_{i,j}} \forall (i,j) \in conex(i,j) \text{ and } \in nofail(i,j,t,s), \forall t, \forall s \tag{6}$$

$$Fl_{i,j,t,s} = 0 \forall (i,j) \in fail(i,j,t,s), \forall t, \forall s \tag{7}$$

$$-\overline{Fl_{i,j}} \le Fl_{i,j,t,s} \le \overline{Fl_{i,j}} \forall (i,j) \in conex(i,j) \text{ and } \in nofail(i,j,t,s), \forall t, \forall s \tag{8}$$

$$\beta_{ref,t,s} = 0 \forall t, \forall s \tag{9}$$

$$-\frac{\pi}{2} \le \beta_{i,t,s} \le \frac{\pi}{2} \forall i, \forall t, \forall s \tag{10}$$

Constraints (11) are nodal electric power balance equations; they make sure that at each bus, time and scenario sum of power generated by FC, PV power plants, dispatchable generators, discharging power of fixed and mobile batteries and electricity shed is equal to sum of electricity demand, electric power fed into the connected electrolyzer, charging power of fixed and mobile batteries and power outflow of the bus. Constraints (12) ensure the adequacy of hydrogen at system buses, according to which, for each bus, at each time and scenario, sum of the hydrogen produced by electrolyzer, hydrogen outflow of hydrogen storage tank and hydrogen shed should not be less than nodal hydrogen demand, hydrogen fed into FC and hydrogen inflow of hydrogen storage tank. Constraints (13) bound the nodal electric demand shed to the nodal electric demand and similarly, constraints (14) bound the nodal hydrogen shed to the nodal hydrogen demand.

$$P_{FC,i,t,s} + P_{MB,dch,i,t,s} + P_{dch,bat,i,t,s} + \sum_{g \in \Lambda_i^g} P_{g,t,s} + \sum_{PV \in \Lambda_i^{PV}} P_{PV,t,s} + P_{shed,i,t,s} = D_{e,i,t} + P_{EL,i,t,s} + P_{MB,ch,i,t,s} + P_{ch,bat,i,t,s} + \sum_{j \in \Omega_i^{connectbus}} P_{i,j,t,s} \forall i, \forall t, \forall s \tag{11}$$

$$H_{EL,i,t,s} + H_{dch,tank,i,t,s} + H_{shed,i,t,s} \ge D_{h,i,t} + H_{ch,tank,i,t,s} + H_{FC,i,t,s} \forall i, \forall t, \forall s \tag{12}$$

$$P_{shed,i,t,s} \le D_{e,i,t} \forall i, \forall t, \forall s \tag{13}$$

$$H_{shed,i,t,s} \le D_{h,i,t} \forall i, \forall t, \forall s \tag{14}$$

The constraints of the dispatchable generators are represented as constraints (15)–(18) [28], among which Eqs. (15)–(16) represent ramp-up and ramp-down rate limits that preclude the stress on rotors. Constraints (17) ensure that the generating power of online dispatchable generators is confined within their corresponding allowed operation interval and constraints (18) define $u_{g,t,s}$ which denote the online/offline status of dispatchable generators as binary variables [29,30].

$$P_{g,t+1,s} - P_{g,t,s} \le RU_g \forall g, \forall t, \forall s \tag{15}$$

$$P_{g,t-1,s} - P_{g,t,s} \le RD_g \forall g, \forall t, \forall s \tag{16}$$

$$\underline{P_g} u_{gen,t,s} \le P_{g,t,s} \le \overline{P_g} u_{g,t,s} \forall g, \forall t, \forall s \tag{17}$$

$$u_{g,t,s} \in \{0,1\} \forall g, \forall t, \forall s \tag{18}$$

The operation of fixed batteries must respect constraints (19)–(23) [31]. Constraints (19) and (20) respectively confine the charging and discharging power of batteries within their corresponding allowed range. Constraints (21) do not allow the SOC of batteries either exceed their upper bounds or go below their lower bounds. Constraints (22) do not allow simultaneous charge and discharge of batteries. Constraints (23) represent the changes in SOC of batteries over time, which is a function of their charging power and discharging power [32–34].

$$\underline{P_{dch,bat,i}} u_{dch,bat,i,t,s} \le P_{dch,bat,i,t,s} \le \overline{P_{dch,bat,i}} u_{dch,bat,i,t,s} \forall i, \forall t, \forall s \tag{19}$$

$$\underline{P_{ch,bat,i}} u_{ch,bat,i,t,s} \le P_{ch,bat,i,t,s} \le \overline{P_{ch,bat}} u_{ch,bat,i,t,s} \forall i, \forall t, \forall s \tag{20}$$

$$\underline{E_{bat,i}} \le E_{bat,i,t,s} \le \overline{E_{bat,i}} \forall i, \forall t, \forall s \tag{21}$$

$$u_{ch,bat,i,t,s} + u_{dch,bat,i,t,s} \le 1 \forall i, \forall t, \forall s \tag{22}$$

$$E_{bat,i,t,s} = E_{bat,i,t-1,s} + \eta_{ch,bat} P_{ch,bat,i,t,s} \Delta t - \left(\frac{P_{dch,bat,i,t,s}}{\eta_{dch,bat}}\right) \Delta t \forall i, \forall s \tag{23}$$

The operation of mobile batteries is subject to constraints (24)–(29) [26]. As mobile batteries must be installed at suitable buses to enhance the resilience of the system, they may be either in discharge or idle states. Constraints (24) are nonlinear, due to the existence of the product of binary terms. Since solving a nonlinear model is a big challenge, we have transformed the nonlinear constraints (24) into (24.a) to (24.e). Constraint (28) ensures that the number of installed mobile batteries is equal to the number of available mobile batteries.

$$\underline{P_{MB,dch}} u_{MB,dch,i,t,s} \mu_{MB,i} \le P_{MB,dch,i,t,s} \le \overline{P_{MB,dch}} u_{MB,dch,i,t,s} \mu_{MB,i} \forall i, \forall t, \forall s \tag{24}$$

$$\underline{E_{MB}} \le E_{MB,i,t,s} \le \overline{E_{MB}} \forall i, \forall t, \forall s \tag{25}$$

$$u_{MB,dch,i,t,s} \in \{0,1\} \forall i, \forall t, \forall s \tag{26}$$

$$E_{MB,i,t,s} = E_{MB,i,t-1,s} - \Delta t \left(\frac{P_{MB,dch,t,s}}{\eta_{MB,dch}}\right) \forall i, \forall t, \forall s \tag{27}$$

$$\sum_i \mu_{MB,i} = N_{MB} \tag{28}$$

$$\mu_{MB,i} \in \{0,1\} \forall i \tag{29}$$

$$\underline{P_{MB,dch}} Z_{MB,dch,i,t,s} \le P_{MB,dch,i,t,s} \le \overline{P_{MB,dch}} Z_{MB,dch,i,t,s} \forall i, \forall t, \forall s \tag{24.a}$$

$$z_{MB,dch,i,t,s} \le \mu_{MB,i} \forall i, \forall t, \forall s \tag{24.b}$$

$$z_{MB,dch,i,t,s} \le u_{MB,dch,i,t,s} \forall i, \forall t, \forall s \tag{24.c}$$

$$z_{MB,dch,i,t,s} \ge u_{MB,dch,i,t,s} + \mu_{MB,i} - 1 \forall i, \forall t, \forall s \tag{24.d}$$

$$z_{MB,dch,i,t,s} \in \{0,1\} \forall i, \forall t, \forall s \tag{24.e}$$

Constraints of electrolyzers are represented by Eqs. (30)–(34). As per Eq. (30), the hydrogen produced by an electrolyzer is proportional to its input electricity and its conversion ratio. Constraints (31)–(32) represent ramp-up and ramp-down rate limits of electrolyzers. Constraints (33) ensure that the produced hydrogen of online electrolyzers is confined within their corresponding allowed operation interval and constraints (34) define $u_{EL,t,s}$ which represent the status of electrolyzers as binary variables [35].

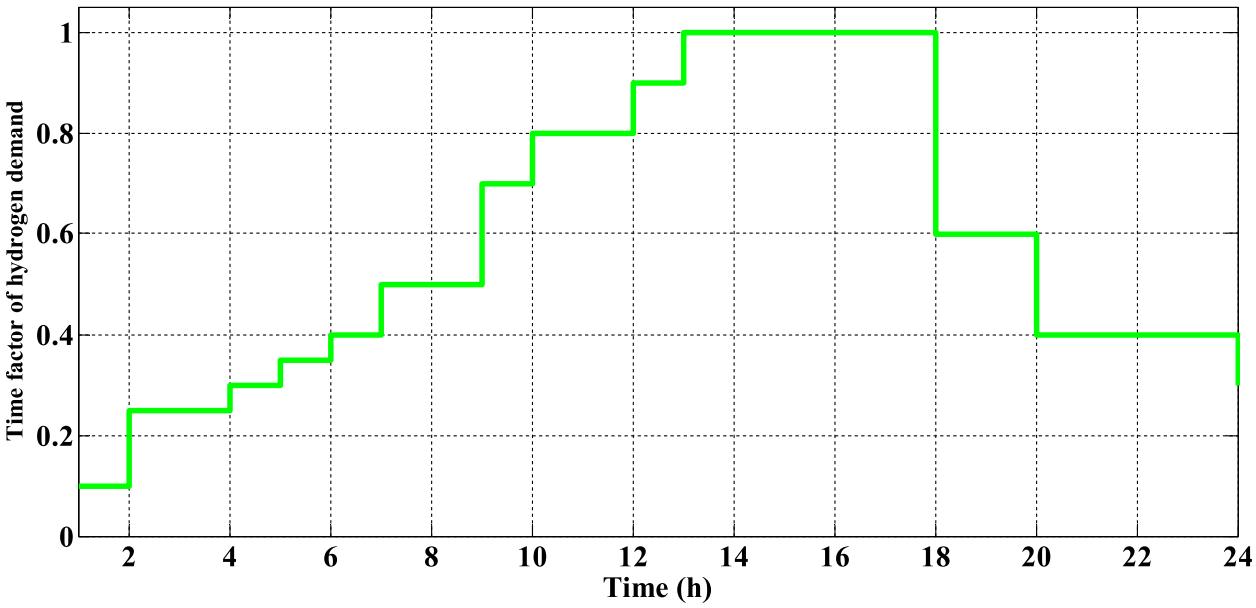

Fig. 2. Time factor of hydrogen demands (normalised values).

$$H_{EL,i,t,s} = CR_{EL}\ P_{EL,i,t,s}\Delta t \forall i, \forall t, \forall s \tag{30}$$

$$H_{EL,i,t+1,s} - H_{EL,i,t,s} \le RU_{EL} \forall i, \forall t, \forall s \tag{31}$$

$$H_{EL,i,t-1,s} - H_{EL,i,t,s} \le RD_{EL} \forall i, \forall t, \forall s \tag{32}$$

$$\underline{H_{EL}} u_{EL,i,t,s} \le H_{EL,i,t,s} \le \overline{H_{EL}} u_{EL,i,t,s} \forall i, \forall t, \forall s \tag{33}$$

$$u_{EL,i,t,s} \in \{0,1\} \forall i, \forall t, \forall s \tag{34}$$

FC's constraints are represented by Eqs. (35)–(39). As per Eq. (35), the electricity produced by any FC is proportional to its input hydrogen and its conversion ratio. Constraints (36)–(37) do not let sudden severe changes in electricity generation of FCs. Constraints (38) ensure that the generated electricity of the committed FCs is confined within their corresponding operation interval and constraints (39) define $u_{FC,t,s}$ which denote the status of FCs as binary variables.

$$P_{FC,i,t,s} = \frac{CR_{FC}\ H_{FC,i,t,s}}{\Delta t} \forall i, \forall t, \forall s \tag{35}$$

$$P_{FC,i,t+1,s} - P_{FC,i,t,s} \le RU_{FC} \forall i, \forall t, \forall s \tag{36}$$

$$P_{FC,i,t-1,s} - P_{FC,i,t,s} \le RD_{FC} \forall i, \forall t, \forall s \tag{37}$$

$$\underline{P_{FC}} u_{FC,i,t,s} \le P_{FC,i,t,s} \le \overline{P_{FC}} u_{FC,i,t,s} \forall i, \forall t, \forall s \tag{38}$$

$$u_{FC,i,t,s} \in \{0,1\} \forall i, \forall t, \forall s \tag{39}$$

The charge and discharge of hydrogen storage tanks in HFSs is subject to the constraints (40)–(43) [35,36]. Constraints ((40), (41)) respectively impose limits on hydrogen inflows and outflows of tank. Constraints (42) prevent the stored hydrogen either exceed its upper bound or go below its lower bound. Constraints (43) represent the changes in SOC of tanks over time, which is a function of their hydrogen inflows and outflows.

$$\underline{H_{dch,tank,i}} \le H_{dch,tank,i,t,s} \le \overline{H_{dch,tank,i}} \forall i, \forall t, \forall s \tag{40}$$

$$\underline{H_{ch,tank,i}} \le H_{ch,tank,i,t,s} \le \overline{H_{ch,tank,i}} \forall i, \forall t, \forall s \tag{41}$$

$$\underline{E_{tank,i}} \le E_{tank,i,t,s} \le \overline{E_{tank,i}} \forall i, \forall t, \forall s \tag{42}$$

$$E_{tank,i,t,s} = E_{tank,i,t-1,s} + \eta_{ch,tank} H_{ch,tank,i,t,s} - \left(\frac{H_{dch,tank,i,t,s}}{\eta_{dch,tank}}\right) \forall i, \forall t, \forall s \tag{43}$$

3. Results and analysis

In this section, the results of the proposed resilience enhancement strategy are presented. Without loss of generality, it is assumed that hurricane is the extreme event which happens. In this paper, the default units for power, energy, hydrogen generation/demand and time are respectively MW, MWh, kg and h. As Fig. 1, case study is a modified IEEE 24-bus power system with 5 PV power plants at buses 1, 2, 13, 15 and 23 respectively with maximum power 1000 MW, 800 MW, 800 MW, 1200 MW and 1500 MW. Five HFSs exist at buses 3, 5, 12, 19 and 22; each HFS contains a PEM electrolyzer, a FC and a hydrogen tank. Hydrogen demands exist at buses 3, 5, 12, 19, 22 respectively with peak 200 kg, 250 kg, 400 kg, 550 kg and 700 kg. There are 3 available mobile batteries which must be used in suitable buses to enhance the resilience of system.

Table 1
Specifics of fixed batteries.

Number	Bus	Maximum SOC	Initial SOC	Minimum charging power	Maximum charging power	Minimum discharging power	Maximum discharging power	Charging efficiency	Discharging efficiency
#1	1	1500	150	10	100	10	100	0.95	0.95
#2	4	850	150	10	200	10	200	0.95	0.95
#3	7	1500	150	10	350	10	350	0.95	0.95
#4	14	2500	150	10	400	10	400	0.95	0.95
#5	15	2500	150	10	400	10	400	0.95	0.95
#6	17	2500	150	10	400	10	400	0.95	0.95
#7	20	2500	150	10	400	10	400	0.95	0.95

Table 2
Specifics of mobile batteries.

Maximum SOC	Initial SOC	Minimum charging power	Maximum charging power	Minimum discharging power	Maximum discharging power	Charging efficiency	Discharging efficiency
1500	1500	2	200	2	200	0.95	0.95

Table 3
Specifics of hydrogen storage systems.

Maximum SOC	Initial SOC	Minimum charging power	Maximum charging power	Minimum discharging power	Maximum discharging power	Charging efficiency	Discharging efficiency
6000	6000	0	1000	0	1000	1	1

Table 4
Introduction of considered scenarios in the stochastic model.

Scenario	Damaged lines	Probability	Isolated buses
1	1–5,5–10 at time interval [2–19], 9–12, 12–23, 10–12, 12–13 at time interval [4,20]	0.3	5, 12
2	3–9,3–1, 3–24 at time interval [1–18], 17–22, 21–22 at time interval [3,14]	0.2	3, 22
3	2–6, 6–10 at time interval [5,16], 1–5, 5–10 at time interval [5,16], 9–12, 12–23, 10–12, 12–13 at time interval [6,20]	0.1	5, 6, 12
4	3–9, 3–1, 3–24 at time interval [4,16], 19–20 at time interval [4,16]	0.1	3
5	1–5,5–10 at time interval [8–20], 19–20 at time interval [8–20],	0.1	5
6	3–9,3–1, 3–24 at time interval [5–17], 20–23, 6–10 at time interval [5–17],	0.1	3
7	1–5,5–10 at time interval [2–24], 15–24 at time interval [2–24]	0.05	5
8	2–6, 6–10 at time interval [5,23], 20–23 at time interval [1–24]	0.05	6

Power system data may be found in [26].

It is assumed that in electrolyzer, 1 MWh electricity is converted to 25 kg hydrogen and in FC, 1 kg hydrogen is converted to 0.005 MWh (5 kW) electricity [37]. Assuming value of 1 kg hydrogen and 1 kWh electricity as 6$ and 0.15$ respectively, the normalised weights in the developed multi-objective model have been respectively set as 0.96 and 0.04 for ELNS of electricity and hydrogen. Minimum and maximum power of FCs are 0 MW and 2 MW and their ramp rates are 2 MW. Minimum and maximum power of electrolyzers are 0 MW and 500 MW and their ramp rates are 200 MW. Minimum and maximum power of both dispatchable generators are 100 MW and 1200 MW and their ramp rates are 100 MW. To see how the hydrogen demand of the system changes over time, have a look at Fig. 2. Specifics of fixed batteries, mobile batteries and hydrogen storage systems have been respectively included in Tables 1–3. Minimum state of charge (SOC) of all storage systems is 0. The details of 8 selected scenarios in the developed stochastic model can be seen in Table 4.

As per the achieved results, with the proposed resilience enhancement strategy, ELNS of electricity is 287.35 MWh and ELNS of hydrogen is 0 kg. The results show that with the proposed resilience enhancement strategy, hurricane does not result in any shed for hydrogen demands in buses of the system. Optimal location of mobile batteries are buses 3, 5 and 6. Mobile batteries, hydrogen tanks and FCs are the cornerstones of the proposed resilience enhancement strategy for HFS-integrated power systems. As per Table 4, hurricane may cause the isolation of some buses in the power system. In scenario 1, buses 5 and 12, in scenario 2, buses 3 and 22, in scenario 3, buses 5, 6, 12 are isolated and in scenarios 4–8, buses 3, 5, 3, 5 and 6 are respectively isolated. In the absence of mobile batteries and FCs, electricity demand of an isolated bus remains fully unsupplied. A mobile battery, installed at a certain bus may release its stored electricity to partially or fully supply local demands. Mobile battery may also feed the electrolyzer of an isolated bus to facilitate hydrogen production and partial/full supply of local hydrogen demands; therefore, mobile battery is expected to enhance ELNS for both electricity and hydrogen demands.

In buses with hydrogen tank and FC, when the bus is isolated, FC may use the hydrogen released by hydrogen tank to produce electricity and supply a portion of local electricity demand. Hydrogen storage may be efficient in resilience enhancement of HFS-integrated power systems. In isolated buses in which the electrolyzer is not able to produce hydrogen, the stored hydrogen may be released to supply at least a portion of local

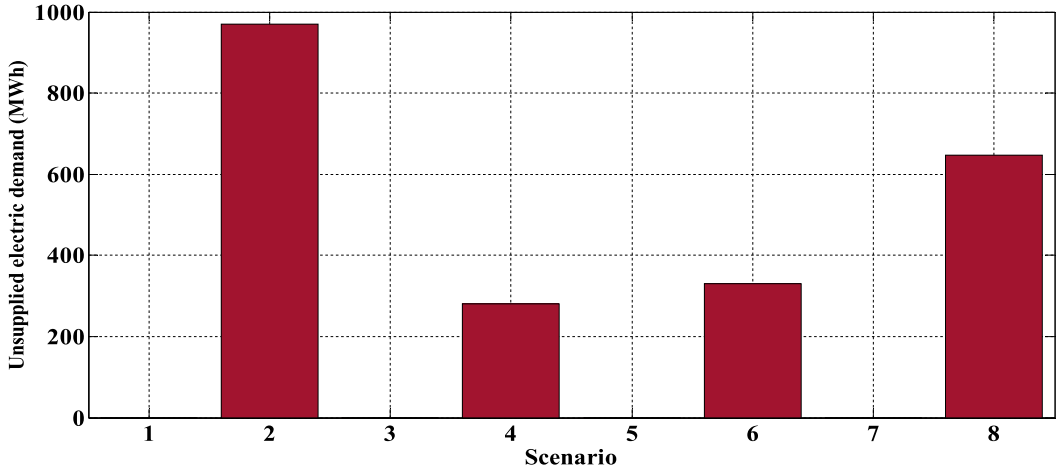

Fig. 3. Total shed of electric demands in different scenarios.

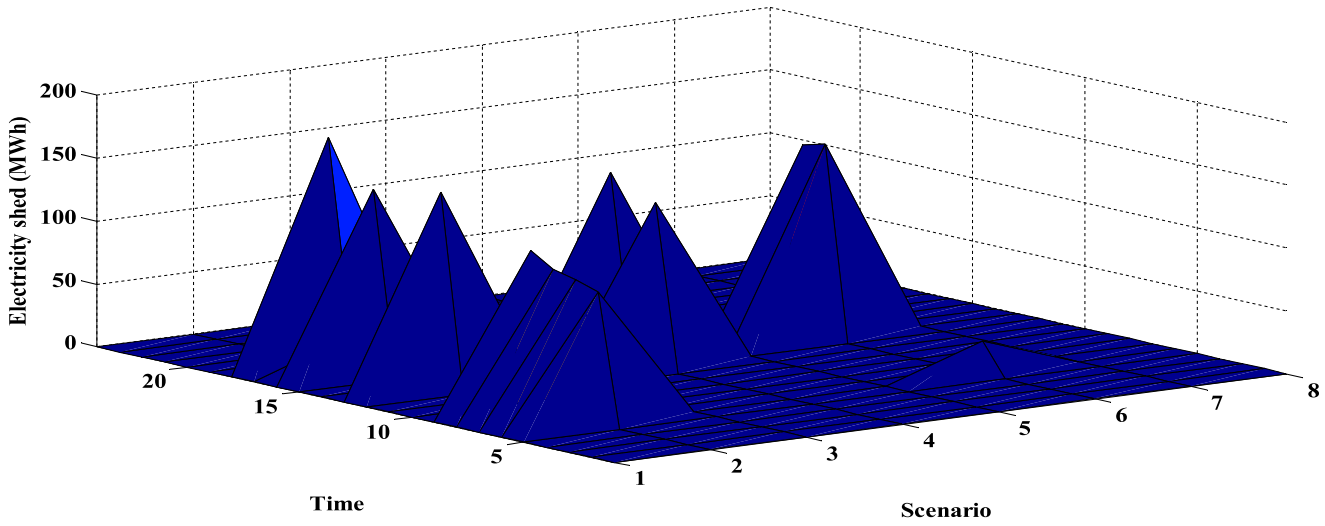

Fig. 4. Electric demand shed at bus 3.

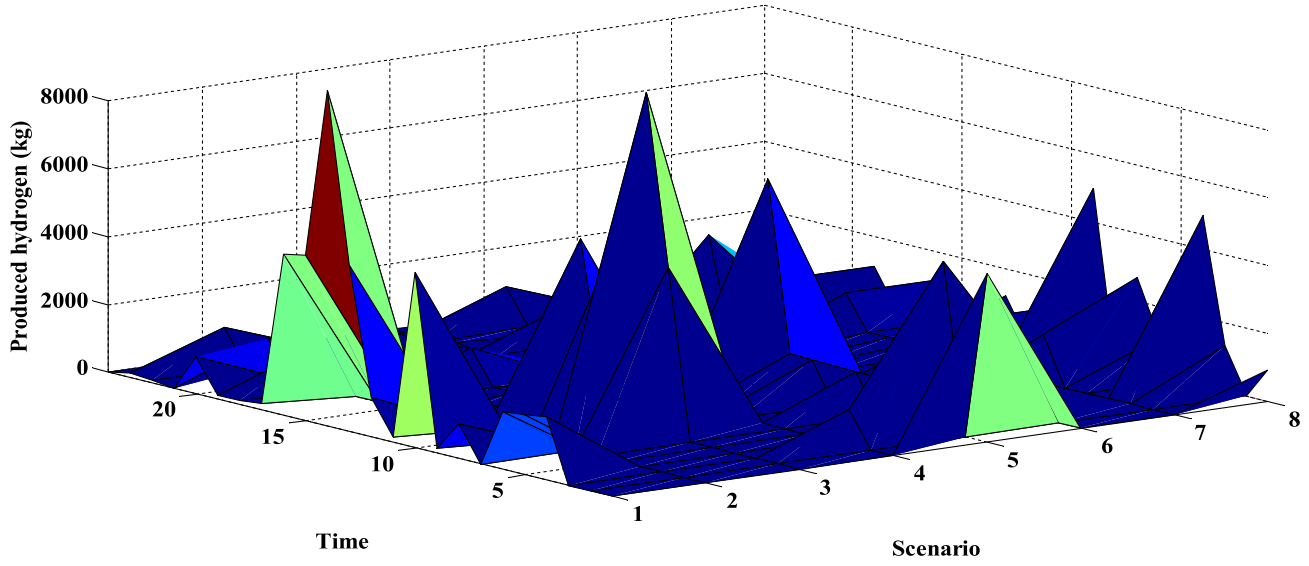

Fig. 5. Hydrogen produced by electrolyzer in bus 3.

hydrogen demands. Hydrogen storage may also improve ELNS of electricity, as its released hydrogen may feed FC and the electricity produced by FC may supply the electricity demands of the isolated bus.

Total shed of electric demands in different scenarios may be seen in Fig. 3. Note that in scenarios 1, 3, 5 and 7, system experiences neither electricity demand shed nor hydrogen demand shed; this means that mobile batteries, hydrogen tanks and FCs have collectively supplied all electricity and hydrogen demands of all isolated buses. On the other hand, scenario 2 with 969.630 MWh experiences the maximum electricity shed as buses 3 and 22 with considerable electricity and hydrogen demands are isolated in this scenario. Electric demand shed of bus 3 at different times and scenarios have been illustrated in Fig. 4. Fig. 5 illustrates the hydrogen produced by electrolyzer in bus 3.

Input and output hydrogen of hydrogen tank, located at bus 3, at different times and scenarios have been respectively illustrated in Figs. 6 and 7. The variations of electricity produced by FC at bus 3 over times and scenarios can be seen in Fig. 8. Discharging power of mobile battery at bus 3 has been illustrated as Fig. 9. In each scenario, the schedule of mobile batteries, hydrogen storage tanks and FCs are set in a way to minimise ELNS of electricity and hydrogen. Note that the locations of mobile batteries are here-and-now scenario-independent decision variables.

To find the share of mobile batteries, FCs and hydrogen tanks on resilience of the studied HFS-integrated power system, see Figs. 10 and 11 which respectively show ELNS of electricity and hydrogen. Fig. 11 shows that if the system contains hydrogen tanks, no hydrogen demand shed occurs in the system; otherwise, system experiences a hydrogen shed of at least 3194 kg. The figures show that mobile batteries are the most efficient tools in resilience enhancement of this HFS-integrated power system. While in the absence of FCs, tanks and mobile batteries, ELNS of electricity and hydrogen were respectively 2027.35 MWh and 5587 kg, the incorporation of mobile batteries reduces them respectively to 317.22 MWh and 3210 kg, which indicates 84 % improvement in ELNS of electricity and 43 % improvement in ELNS of hydrogen. The results show that besides mobile batteries, hydrogen storage tanks and FCs are the most efficient components in resilience enhancement of the system. Hydrogen tanks decrease ELNS of electricity from 2027.35 MWh to 1990.82 MWh, which shows an improvement of 1.8 %; they remove the need of system operator to shed hydrogen demands. FCs improve ELNS of electricity from 2027.35 MWh to 2022.81 MWh, which shows an improvement of 4.54 MWh; although they cause a minor deterioration in ELNS of hydrogen, as they use hydrogen for

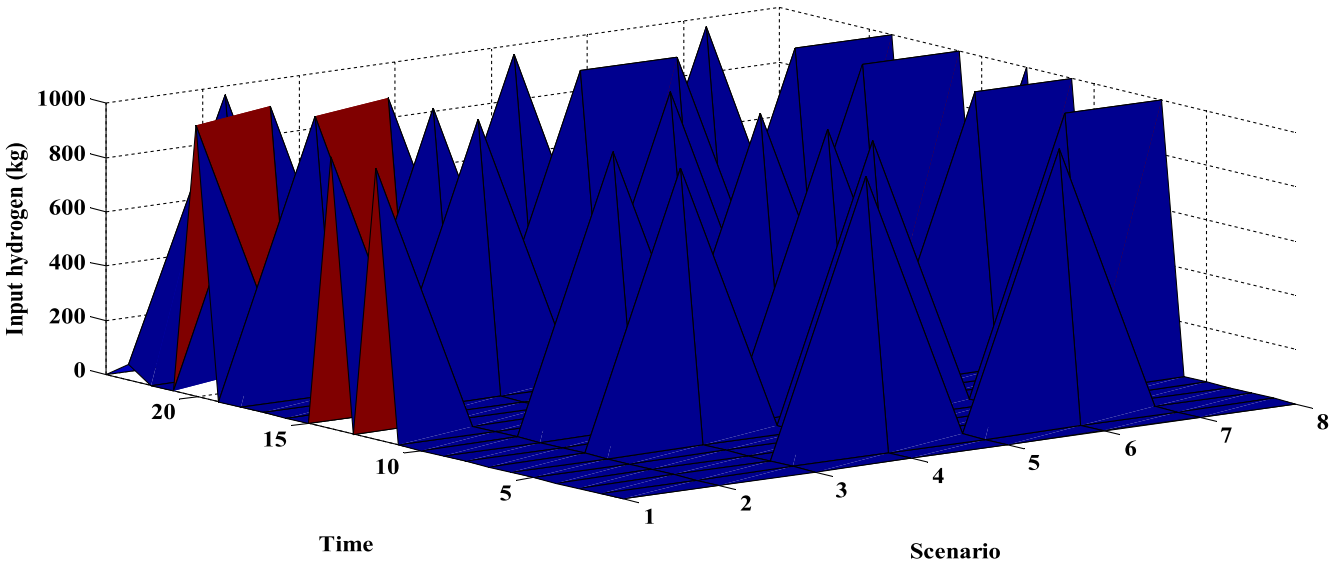

Fig. 6. Hydrogen input of hydrogen tank in bus 3.

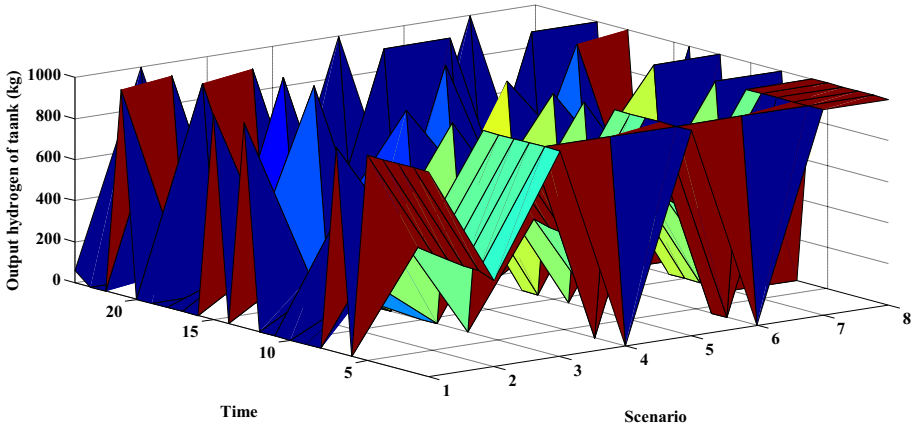

Fig. 7. Hydrogen output of hydrogen tank in bus 3.

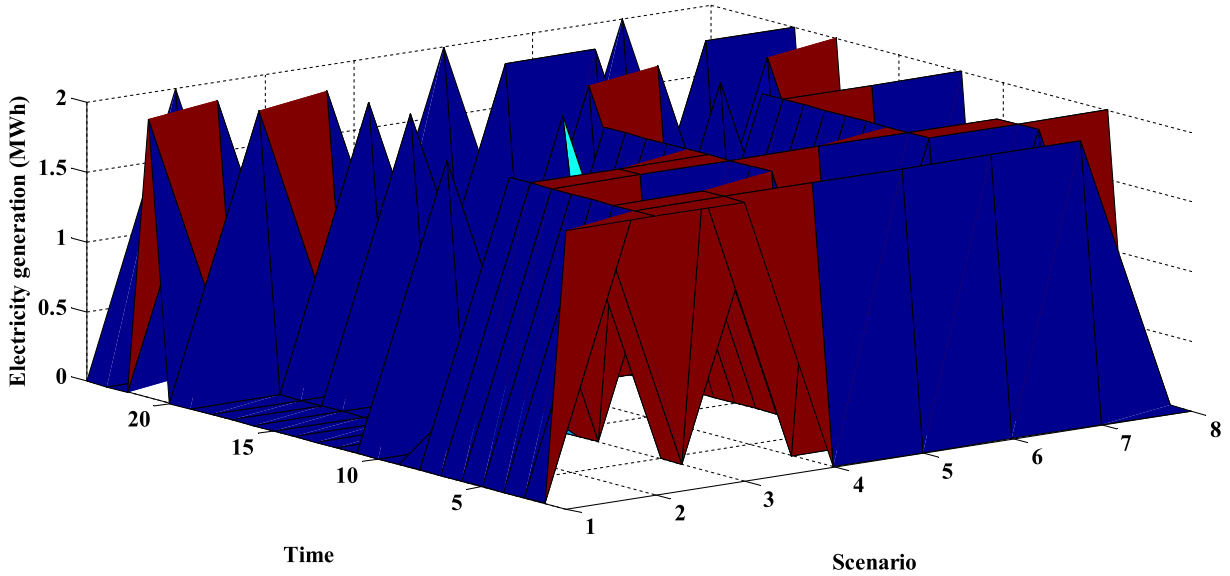

Fig. 8. Electricity produced by FC in bus 3.

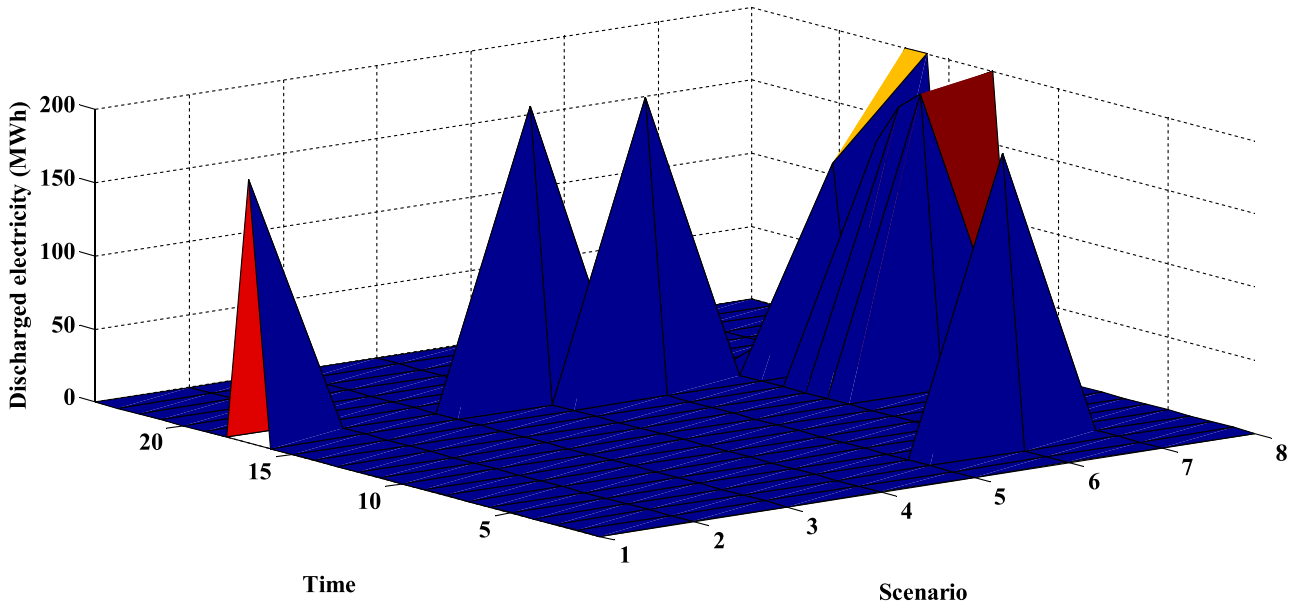

Fig. 9. Discharging power of mobile battery at bus 3.

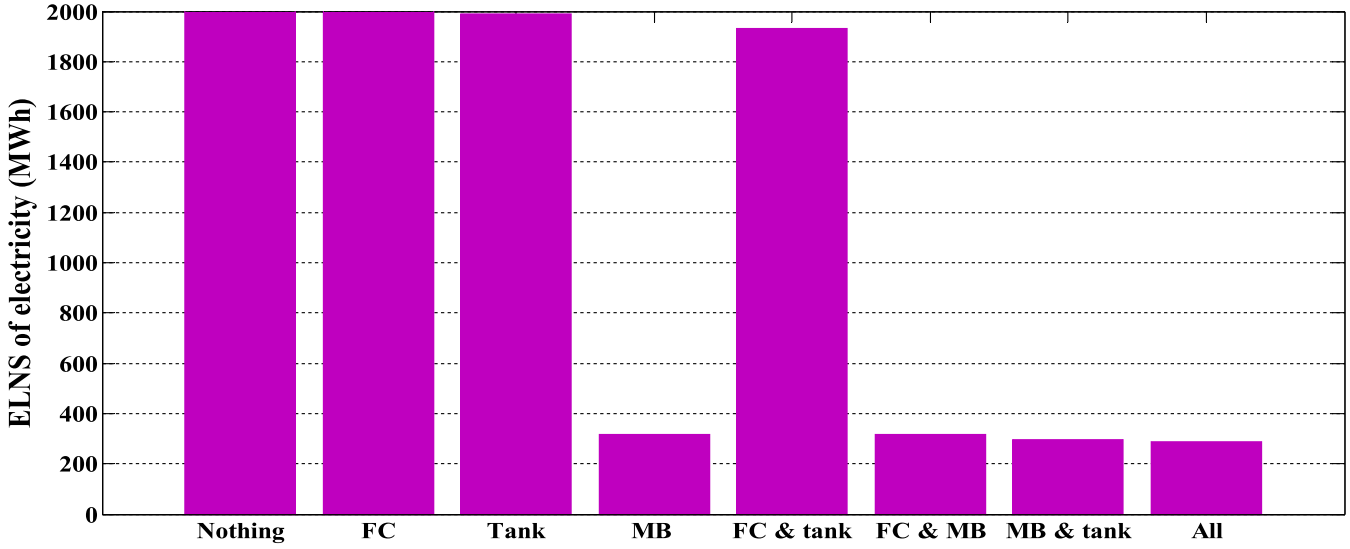

Fig. 10. ELNS of electricity for different cases.

electricity production.

Here, a sensitivity analysis is done to see how the results of the developed model are sensitive to its parameters; sensitivity analysis is done with respect to size of FCs, hydrogen storage tanks and mobile batteries, number of mobile batteries as well as the weights of ELNSs. The sensitivity of system resilience to size of FCs can be seen in Fig. 12 which shows that the increase of FC size beyond 2 MW leads to no improvement in resilience of the system. With any FCs' size, even without FC, ELNS of hydrogen is zero. Figs. 13 and 14 respectively show the sensitivity of ELNS of electricity and hydrogen to the size of hydrogen tanks. According to these figures, in order to remove the necessity of hydrogen demands, the capacity of hydrogen tanks must be at least 6000 kg. With 5000 kg tanks, ELNS of electricity would be 287.35 MWh. An increase of tank capacity from 6000 kg to 7000 kg improves ELNS of electricity by only 0.7 % and does not change ELNS of hydrogen; so, 6000 kg seems to be a good choice for size of hydrogen tanks.

The sensitivity of system resilience to the size and number of available mobile batteries may be seen as Figs. 15 and 16. With all sizes of mobile batteries, system experiences no hydrogen demand shed. As per Fig. 15, while with 2000 MWh mobile batteries, the system experiences an ELNS of 107.47 MWh for electricity, 3000 MWh mobile batteries remove the necessity of either electricity or hydrogen demand shed throughout the system. Fig. 16 shows that adding the second mobile battery improves ELNS of electricity by 55 % and adding the third one causes a further 42 % improvement in ELNS of electricity. Fig. 16 also indicates that increasing the number of mobile batteries beyond 3 leads to no improvement in ELNS.

As the weights of objectives in multi-objective optimisation models affect the optimal objectives, a sensitivity analysis has been done to measure the sensitivity of ELNS of electricity and hydrogen to weights. As per the results, the sensitivity of ELNS of electricity to weights is negligible. Fig. 17 shows the effect of weights in the developed bi-objective model on ELNS of hydrogen. According to this figure, the weights equal to or above 0.005 for ELNS of hydrogen, removes the necessity of hydrogen demand shed throughout the system.

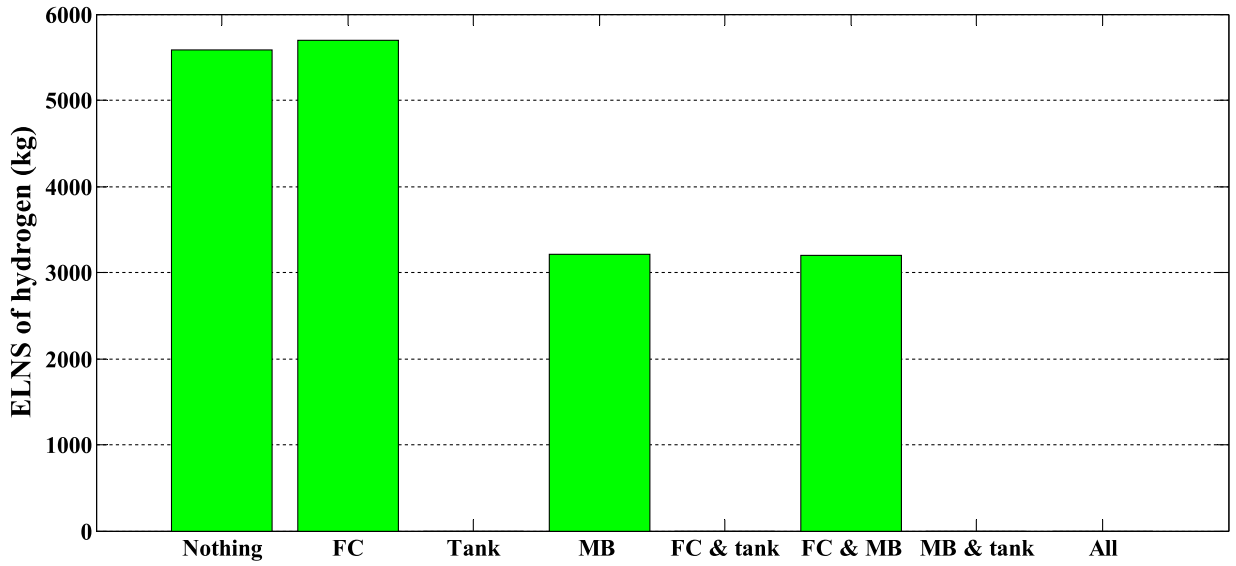

Fig. 11. ELNS of hydrogen for different cases.

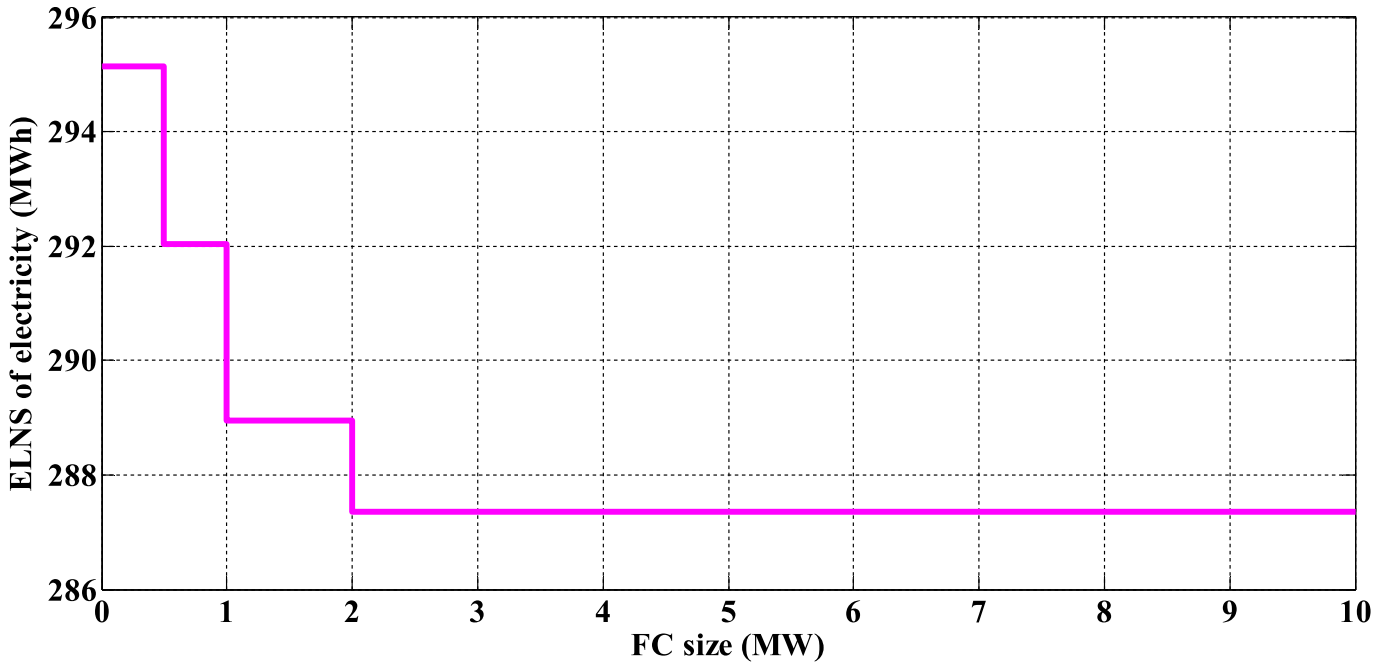

Fig. 12. Effect of FCs' size on ELNS of electricity.

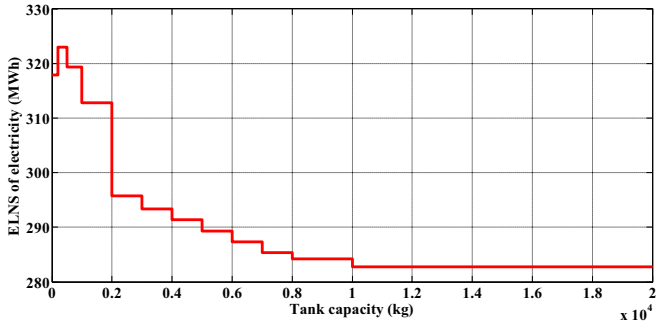

Fig. 13. Effect of size of tanks on ELNS of electricity.

4. Conclusions

In this research, a novel strategy based on mobile batteries, FCs and hydrogen tanks has been proposed for resilience enhancement of HFS-integrated power systems with high PV penetration, considering the uncertainties in the failed lines, failure times and repair times. A two-stage stochastic model has been developed in which the locations of mobile batteries are first-stage here-and-now decision variables and other variables are second-stage wait-and-see decision variables.

The results show that thanks to the proposed resilience enhancement strategy, hurricane does not result in any shed for hydrogen demands; as per the results, mobile batteries and then hydrogen tanks and FCs are the most efficient tools in resilience enhancement of the studied system. Mobile batteries cause 84 % improvement in ELNS of electricity and 43 % improvement in ELNS of hydrogen; they release their stored

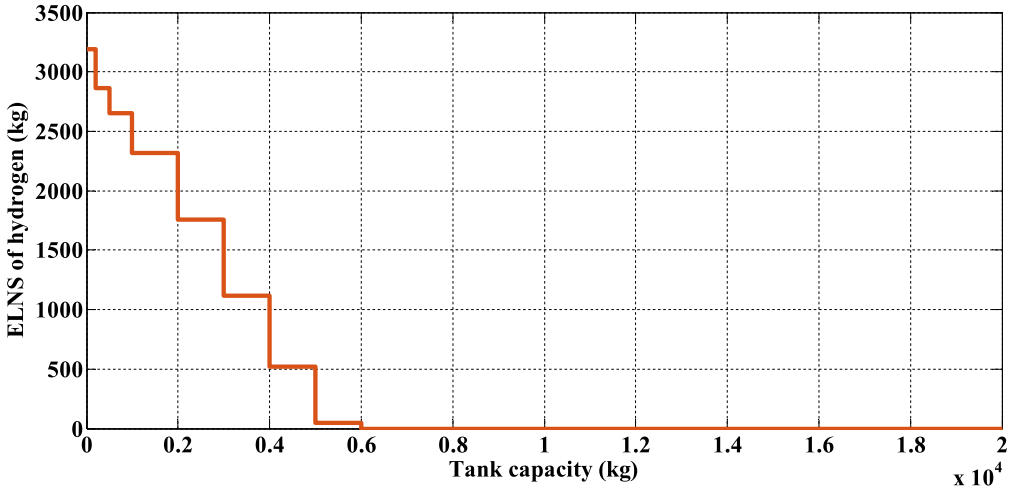

Fig. 14. Effect of size of tanks on ELNS of hydrogen.

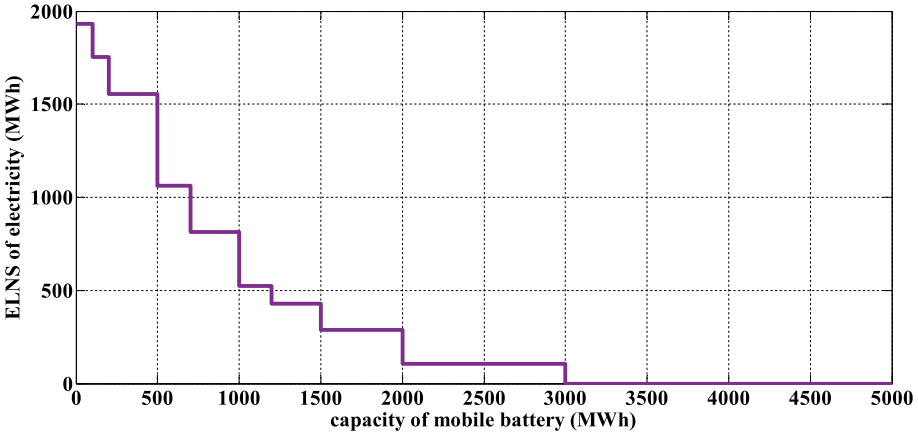

Fig. 15. Effect of size of mobile batteries on ELNS of electricity.

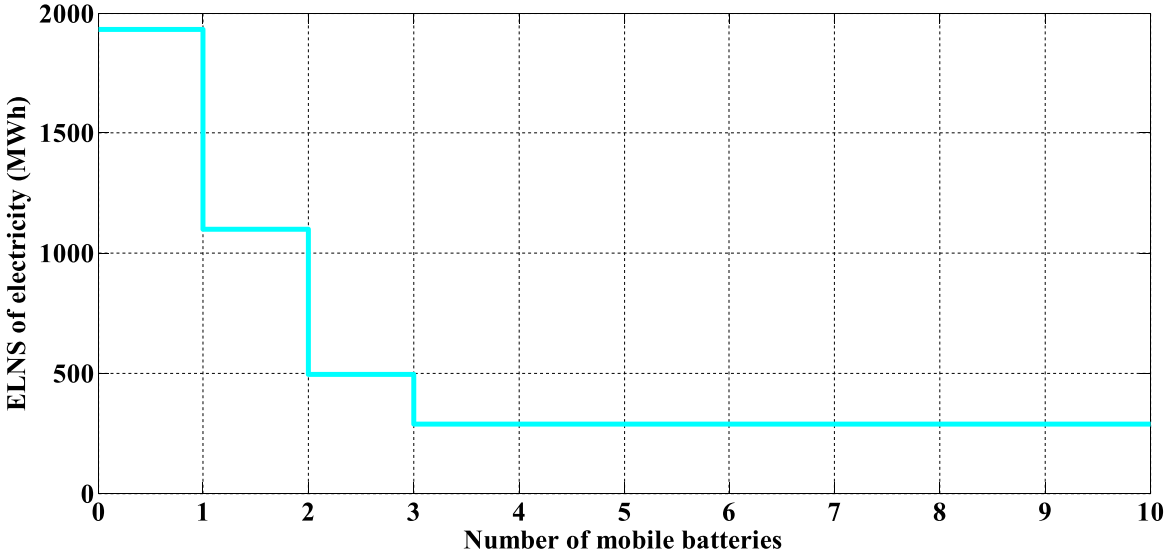

Fig. 16. Effect of the number of mobile batteries on ELNS of electricity.

electricity to supply demands in isolated buses; they may also feed the electrolyzer of isolated buses to facilitate hydrogen production and supply of local hydrogen demands. Hydrogen tanks decrease ELNS of electricity from 2027.35 MWh to 1990.82 MWh, which shows an improvement of 1.8 % and remove the need of system operator for hydrogen shed. In isolated buses in which the electrolyzer is not able to

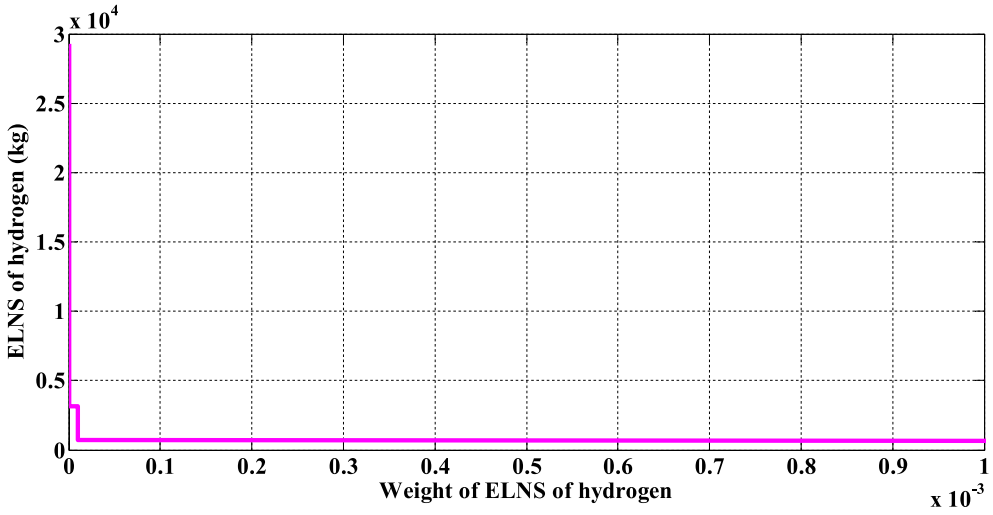

Fig. 17. Effect of the weights on ELNS of hydrogen.

produce hydrogen, the stored hydrogen is released to supply local hydrogen demands. Hydrogen tanks also improve ELNS of electricity, as their released hydrogen feeds FC and the electricity produced by FC supplies the electricity demands of the isolated bus. FCs improve ELNS of electricity by 4.54 MWh; although they cause a minor deterioration in ELNS of hydrogen.

A sensitivity analysis has been done with respect to size of FCs, hydrogen storage tanks and mobile batteries, number of mobile batteries as well as the weights of ELNSs. The results show that the increase of FCs' size beyond 2 MW leads to no improvement in resilience of the system and with any FC size, ELNS of hydrogen is zero. According to the results, to remove the necessity of hydrogen demands, the capacity of hydrogen tanks must be at least 6000 kg. An increase of tank capacity from 6000 kg to 7000 kg improves ELNS of electricity by only 0.7 % and does not change ELNS of hydrogen; so, 6000 kg seems to be a good choice for size of hydrogen tanks.

As per sensitivity analysis, with 2000 MWh mobile batteries, the system experiences an ELNS of 107.47 MWh for electricity, whereas 3000 MWh mobile batteries remove the necessity of either electricity or hydrogen demand shed throughout the system. The results show that adding the second mobile battery improves ELNS of electricity by 55 % and adding the third one causes a further 42 % improvement in ELNS of electricity. Increasing the number of mobile batteries beyond 3 leads to no improvement in ELNS. As per the results, the sensitivity of ELNS of electricity to weights is negligible and the weights equal to or above 0.005 for ELNS of hydrogen, remove the necessity of hydrogen demand shed.

CRediT authorship contribution statement

Wenqing Cai Conceptualization, Methodology, Software, Validation, Writing and Editing.

Seyed Amir Mansouri Conceptualization, Methodology, Software, Validation, Writing- Reviewing and Editing.

Ahmad Rezaee Jordehi Conceptualization, Methodology, Software, Validation, Writing- Reviewing and Editing.

Marcos Tostado-Véliz Conceptualization, Methodology, Software, Validation, Writing- Reviewing and Editing.

Amir Ahmarinejad Original draft preparation, Visualization, Reviewing and Editing, Discussion.

Francisco Jurado Reviewing and Editing, Discussion.

Declaration of competing interest

The authors declare that they have no known competing financial interests or personal relationships that could have appeared to influence the work reported in this paper.

Data availability

Data will be made available on request.

References

[1] T. Holm, T. Borsboom-Hanson, O.E. Herrera, W. Mérida, Hydrogen costs from water electrolysis at high temperature and pressure, Energ. Conver. Manage. 237 (2021), 114106.
[2] G. Matute, J.M. Yusta, J. Beyza, L.C. Correas, Multi-state techno-economic model for optimal dispatch of grid connected hydrogen electrolysis systems operating under dynamic conditions, Int. J. Hydrogen Energy 46 (2021) 1449–1460.
[3] R. Hemmati, H. Mehrjerdi, M. Bornapour, Hybrid hydrogen-battery storage to smooth solar energy volatility and energy arbitrage considering uncertain electrical-thermal loads, Renew. Energy 154 (2020) 1180–1187.
[4] E. Taibi, R. Miranda, W. Vanhoudt, T. Winkel, J.-C. Lanoix, F. Barth, Hydrogen From Renewable Power: Technology Outlook for the Energy Transition, 2018.
[5] Y. Tao, J. Qiu, S. Lai, J. Zhao, Integrated electricity and hydrogen energy sharing in coupled energy systems, IEEE Trans. Smart Grid 12 (2020) 1149–1162.
[6] H. Ishaq, I. Dincer, C. Crawford, A review on hydrogen production and utilization: challenges and opportunities, Int. J. Hydrogen Energy 47 (2022) 26238–26264.
[7] G.K. Karayel, N. Javani, I. Dincer, Green hydrogen production potential for Turkey with solar energy, Int. J. Hydrogen Energy 47 (2022) 19354–19364.
[8] M. Yu, K. Wang, H. Vredenburg, Insights into low-carbon hydrogen production methods: green, blue and aqua hydrogen, Int. J. Hydrogen Energy 46 (2021) 21261–21273.
[9] M. Younas, S. Shafique, A. Hafeez, F. Javed, F. Rehman, An overview of hydrogen production: current status, potential, and challenges, Fuel 316 (2022), 123317.
[10] S. Bahou, Techno-economic assessment of a hydrogen refuelling station powered by an on-grid photovoltaic solar system: a case study in Morocco, Int. J. Hydrogen Energy (2023).
[11] A. Rezaee Jordehi, S.A. Mansouri, M. Tostado Veliz, M.J. Hossain, M. Nasir, F. Jurado, Optimal placement of hydrogen fuel stations in power systems with high photovoltaic penetration and responsive electric demands in presence of local hydrogen markets, Int. J. Hydrog. Energy (2023), https://doi.org/10.1016/j.ijhydene.2023.07.132.
[12] A. Rezaee Jordehi, S.A. Mansouri, M. Tostado Veliz, M.J. Hossain, M. Carrión, F. Jurado, A risk-averse two-stage stochastic model for optimal participation of hydrogen fuel stations in electricity markets, Int. J. Hydrogen Energy (2023), https://doi.org/10.1016/j.ijhydene.2023.07.197.
[13] A. Mansouri, A. Rezaee Jordehi, M. Marzband, M. Tostado Veliz, F. Jurado, J. Aguado, An IoT-enabled hierarchical decentralized framework for multi-energy microgrids market management in the presence of smart prosumers using a deep learning-based forecaster, Applied Energy 333 (2023).
[14] M. Gökçek, C. Kale, *Optimal design of a hydrogen refuelling station (HRFS) powered by hybrid power system*, Energy Conv. Manage. 161 (2018) 215–224.
[15] A. Rabiee, A. Keane, A. Soroudi, Technical barriers for harnessing the green hydrogen: a power system perspective, Renew. Energy 163 (2021) 1580–1587.

[16] A. Rabiee, A. Keane, A. Soroudi, Green hydrogen: a new flexibility source for security constrained scheduling of power systems with renewable energies, Int. J. Hydrogen Energy 46 (2021) 19270–19284.
[17] J. Brey, Use of hydrogen as a seasonal energy storage system to manage renewable power deployment in Spain by 2030, Int. J. Hydrogen Energy 46 (2021) 17447–17457.
[18] G. Kakoulaki, I. Kougias, N. Taylor, F. Dolci, J. Moya, A. Jäger-Waldau, Green hydrogen in Europe–a regional assessment: substituting existing production with electrolysis powered by renewables, Energ. Conver. Manage. 228 (2021), 113649.
[19] Z. Bao, Z. Hu, D. Zhao, Optimal multi-period pricing and operating of hydrogen refueling stations considering the coupling of transportation and power systems, in: 2021 IEEE 5th Conference on Energy Internet and Energy System Integration (EI2), IEEE, 2021, pp. 190–195.
[20] F. Grueger, O. Hoch, J. Hartmann, M. Robinius, D. Stolten, Optimized electrolyzer operation: employing forecasts of wind energy availability, hydrogen demand, and electricity prices, Int. J. Hydrogen Energy 44 (2019) 4387–4397.
[21] J. Li, J. Lin, H. Zhang, Y. Song, G. Chen, L. Ding, D. Liang, Optimal investment of electrolyzers and seasonal storages in hydrogen supply chains incorporated with renewable electric networks, IEEE Trans. Sustain. Energy 11 (2019) 1773–1784.
[22] H. Aki, I. Sugimoto, T. Sugai, M. Toda, M. Kobayashi, M. Ishida, Optimal operation of a photovoltaic generation-powered hydrogen production system at a hydrogen refueling station, Int. J. Hydrogen Energy 43 (2018) 14892–14904.
[23] S. Klyapovskiy, Y. Zheng, S. You, H.W. Bindner, Optimal operation of the hydrogen-based energy management system with P2X demand response and ammonia plant, Appl. Energy 304 (2021), 117559.
[24] A. Rezaee Jordehi, S.A. Mansouri, M. Tostado-Véliz, A. Ahmarinejad, F. Jurado, Resilience-oriented placement of multi-carrier microgrids in power systems with switchable transmission lines, Int. J. Hydrogen Energy (2023), https://doi.org/10.1016/j.ijhydene.2023.40.303.
[25] Z. Bie, Y. Lin, G. Li, F. Li, Battling the extreme: A study on the power system resilience, Proc. IEEE 105 (2017) 1253–1266.
[26] A. Rezaee Jordehi, S.A. Mansouri, M. Tostado-Véliz, A. Iqbal, F. Jurado, Industrial Energy Hubs with Electric, Thermal and Hydrogen Demands for Resilience Enhancement of Mobile Storage-Integrated Power Systems, 2023, https://doi.org/10.1016/j.ijhydene.2023.07.205.
[27] A. Soroudi, Power System Optimization Modeling in GAMS, Springer, 2017.
[28] A.R. Jordehi, A stochastic model for participation of virtual power plants in futures markets, pool markets and contracts with withdrawal penalty, J. Energy Storage 50 (2022), 104334.
[29] A.R. Jordehi, Scheduling heat and power microgrids with storage systems, photovoltaic, wind, geothermal power units and solar heaters, J. Energy Storage 41 (2021), 102996.
[30] A.R. Jordehi, M.S. Javadi, J.P. Catalão, Optimal placement of battery swap stations in microgrids with micro pumped hydro storage systems, photovoltaic, wind and geothermal distributed generators, Int. J. Electr. Power Energy Syst. 125 (2021), 106483.
[31] A.R. Jordehi, Risk-aware two-stage stochastic programming for electricity procurement of a large consumer with storage system and demand response, J. Energy Storage 51 (2022), 104478.
[32] A.R. Jordehi, V.S. Tabar, S. Mansouri, F. Sheidaei, A. Ahmarinejad, S. Pirouzi, Two-stage stochastic programming for scheduling microgrids with high wind penetration including fast demand response providers and fast-start generators, Sustain. Energy, Grids Netw. (2022) 100694.
[33] A.R. Jordehi, Two-stage stochastic programming for risk-aware scheduling of energy hubs participating in day-ahead and real-time electricity markets, Sustain. Cities Soc. 103823 (2022).
[34] A.R. Jordehi, V.S. Tabar, S. Mansouri, M. Nasir, S. Hakimi, S. Pirouzi, A risk-averse two-stage stochastic model for planning retailers including self-generation and storage system, J. Energy Storage 51 (2022), 104380.
[35] M. Nasir, A.R. Jordehi, S.A.A. Matin, V.S. Tabar, M. Tostado-Véliz, S.A. Mansouri, Optimal operation of energy hubs including parking lots for hydrogen vehicles and responsive demands, J. Energy Storage 50 (2022), 104630.
[36] M. Nasir, A.R. Jordehi, M. Tostado-Veliz, V.S. Tabar, S.A. Mansouri, F. Jurado, Operation of energy hubs with storage systems, solar, wind and biomass units connected to demand response aggregators, Sustain. Cities Soc. 103974 (2022).
[37] www.newatlas.com, 2022.